Two-Dimensional Soot

C. M. Sorensen* and W. B. Hageman

Department of Physics and Program for Complex Fluid Flows, Kansas State University, Manhattan, Kansas 66506-2601

Received March 19, 2001. In Final Form: June 11, 2001

Large soot aggregates (ca. 100 μm) in acetylene−air diffusion flames are physically flat and have a fractal dimension of $D = 1.40 \pm 0.04$ consistent with simulations of two-dimensional diffusion-limited cluster aggregation. This occurs because the soot is constrained to a cylindrical annular flame front with a radial thickness that appears thin relative to the increasing dimensions of the soot aggregates, thus confining them to a two-dimensional space during aggregation.

1. Introduction

It is now well established that soot aggregates formed in flames have a fractal morphology.[1−13] A defining relation for fractal aggregates is[11,14]

$$N = k_o(R_g/a)^D \quad (1)$$

where N is the number of primary particles, or monomers, in the aggregate, k_o is a constant of order unity, R_g is the aggregate radius of gyration, and D is the fractal dimension. Numerous examples abound for which eq 1 provides a robust description of soot aggregate morphology and where, without exception, the fractal dimension is found to be in the range of $D = 1.7−1.8$. This universal value is consistent with simulations that show soot aggregation is a diffusion-limited cluster−cluster aggregation (DLCA) process in three-dimensional space.[15−19]

In this paper we provide an exception to the rule that $D = 1.8$ for soot. This comes with very large soot clusters ($\sim$100 μm) formed in an acetylene−air diffusion flame, for which we find $D = 1.40$. This occurs because the soot, which is confined to an annular flame front, becomes larger than the thickness of the flame front and thus sees an effective two-dimensional space. Simulations of two-dimensional DLCA yield fractal aggregates with $D = 1.44$,[18,19] consistent with our measurements.

2. Experimental Methods

2.1. The Flame. An acetylene−air diffusion flame was created by passing acetylene through a variable control flow meter and then vertically out into room air through a 0.9 cm diameter brass tube, as used previously in this laboratory.[13,20] The gas was ignited, and the resulting flame produced a thick soot column due to the incomplete burning of the acetylene fuel. At low flow rates small soot particles ($<$0.3 μm) were produced. These clusters have been found through light scattering analysis to have a fractal dimension of approximately 1.75,[20] which is consistent with three-dimensional DLCA aggregation. However, at higher acetylene flow rates, larger soot particles ($\approx$100 μm, "supersoot") rapidly appeared.[20] These particles were much too large for analysis using optical light scattering.

2.2. Soot Detection Apparatus. The soot particles were large enough so that they could be directly observed and photographed in-situ without disturbing the flame system. To this end a telemicroscope device was used. This device consisted of a 25 mm diameter imaging lens that projected the image of the flame to a 10× microscope objective mounted to a standard 35 mm camera. To freeze the relative upward motion of the soot particles in the flame, a pulsed Nd:YAG laser with 7 ns pulse length was used as a flash lamp. Since the soot particles are effective black bodies and readily absorb light, the flash could not be used to directly illuminate them. Instead, a reflection setup was implemented. The light from the Nd:YAG laser was used, without the aid of any lenses, to illuminate a white background. This illuminated background then, in turn, silhouetted the soot particles and allowed them to be seen through the telemicroscope.

A typical picture obtained through this process is shown in Figure 1. In this photograph the column is seen roughly 8 cm

* Corresponding author. E-mail: sor@phys.ksu.edu.

(1) Sampson, R. J.; Mulholland, G. W.; Gentry, J. W. Structural Analysis of Soot Agglomerates. *Langmuir* **1987**, *3*, 272−281.

(2) Megaridis, C. M.; Dobbins, D. A. Morphological Description of Flame-Generated Materials. *Combust. Sci. Technol.* **1990**, *71*, 95−109.

(3) Zhang, H. X.; Sorensen, C. M.; Ramer, E. R.; Olivier, B. J.; Merklin, J. F. In Situ Optical Structure Factor Measurements of an Aggregating Soot Aerosol. *Langmuir* **1988**, *4*, 867−871.

(4) Gangopadhyay, S.; Elminyawi, I.; Sorensen, C. M. Optical Structure Factor Measurements of Soot Particles in a Premixed Flame. *Appl. Opt.* **1991**, *30*, 4859−4864.

(5) Sorensen, C. M.; Cai, J.; Lu, N. Light-Scattering Measurements of Monomer Size, Monomers Per Aggregate, and Fractal Dimension for Soot Aggregates in Flames. *Appl. Opt.* **1992**, *31*, 6547−6557.

(6) Köylü, U. O.; Faeth, G. M.. Structure of Overfire Soot in Buoyant Turbulent Diffusion Flames at Long Residence Times. *Combust. Flame* **1992**, *89*, 140−156.

(7) Puri, R.; Richardson, T. F.; Santoro, R. J.; Dobbins, R. A. Aerosol Dynamic Processes of Soot Aggregates in a Laminar Ethene Diffusion Flame. *Combust. Flame* **1993**, *92*, 320−333.

(8) Cai, J.; Lu, N.; Sorensen, C. M. Comparison of Size and Morphology of Soot Aggregates as Determined by Light Scattering and Electron Microscope Analysis. *Langmuir* **1993**, *9*, 2861−2068.

(9) Köylü, U. O.; Faeth, G. M. Optical Properties of Overfire Soot in Buoyant Turbulent Diffusion Flames at Long Residence Times. *J. Heat Transfer* **1994**, *116*, 152−159.

(10) Köylü, U. O.; Faeth, G. M. Optical Properties of Soot in Buoyant Laminar Diffusion Flames. *J. Heat Transfer* **1994**, *116*, 971−979.

(11) Cai, J.; Lu, N.; Sorensen, C. M. Analysis of Fractal Cluster Morphology Parameters: Structural Coefficient and Density Autocorrelation Function Cutoff. *J. Colloid Interface Sci.* **1995**, *171*, 470−473.

(12) Köylü, U. O.; Faeth, G. M.; Farias, T. L.; Carvalho, M. G. Fractal and Projected Structure Properties of Soot Aggregates. *Combust. Flame* **1995**, *100*, 621−633.

(13) Sorensen, C. M.; Feke, G. D. The Morphology of Macroscopic Soot. *Aerosol Sci. Technol.* **1996**, *25*, 328−337.

(14) Sorensen, C. M.; Roberts, G. C. The Prefactor of Fractal Aggregates. *J. Colloid Interface Sci.* **1997**, *186*, 447−452.

(15) Meakin, P. Formation of Fractal Clusters and Networks by Irreversible Diffusion-Limited Aggregation. *Phys. Rev. Lett.* **1983**, *51*, 1119−1122.

(16) Kolb, M.; Botet, R.; Jullien, R. Scaling of Kinetically Growing Clusters. *Phys. Rev. Lett.* **1983**, *51*, 1123−1126.

(17) Meakin, P. Fractal Aggregates. *Adv. Colloid Interface Sci.* **1988**, *28*, 249−331.

(18) Jullien, R.; Kolb, M.; Botet, R. *J. Phys., Lett.* **1984**, *45*, L211.

(19) Meakin, P. Off lattice simulations of cluster−cluster aggregation in dimensions 2−6. *Phys. Lett.* **1985**, *107A*, 269.

(20) Sorensen, C. M.; Hageman, W. B.; Rush, T.; Huang, H; Oh, C. Aerogelation in a Flame Soot Aerosol. *Phys. Rev. Lett.* **1998**, *80*, 1782−1785.

10.1021/la0104065 CCC: $20.00
Published on Web 08/07/2001

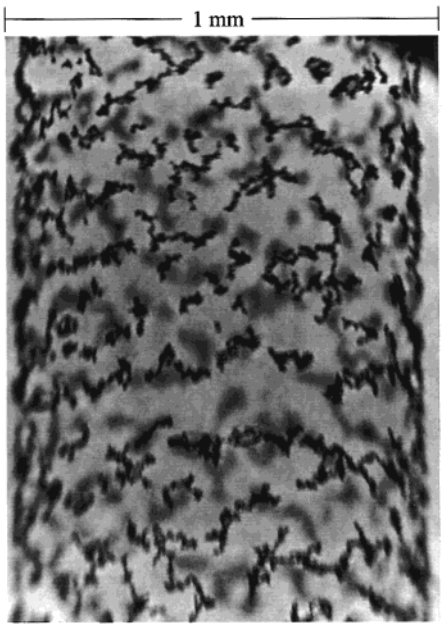

Figure 1. Telemicroscope photograph with a 7 ns flash exposure of the acetylene flame 8 cm above the burner orifice showing supersoot aggregates.

above the base of the flame. This height was chosen well above the glowing combustion region of the flame to minimize light exposure from the hot, glowing soot. At this height the soot column has narrowed to roughly 1 mm in diameter, well down from its 9 mm width at burner level. The soot aggregates have grown to a size of roughly 100 μm in size, up about 4 orders of magnitude from the size of the primary soot monomers. It can also be seen in this picture that the soot particles appear to be held in a thin annulus on the outer edge of the column. No soot was visible within this annulus with the photography. A laser beam directed through the flame scattered greatly from the annulus and much less so from within. We believe this indicates a low concentration of submicron soot within the annulus, an interpretation consistent with previous light scattering measurements.[20] Our view of the aggregates that are in focus on the front side of the soot column (the annulus) becomes foreshortened as it moves to the side of the flame annulus.

Soot particles were also collected by impaction onto glass microscope slides. This was done by holding the slide briefly in the flame with the plane of the slide perpendicular to the flow; i.e., the plane of the slide was horizontal. Figure 2 gives an example of impaction collected soot. We found that thermophoretic collection was not efficient for these supersoot clusters. Photographs of these soot particles were made with an optical microscope.

2.3. Analysis Software for Image Analysis. Photographic images of soot clusters, from either in-situ observation or impaction collection, were digitally scanned using a flatbed scanner at a resolution of 1200 dpi and placed in a bitmap file format. These bitmap images were processed using an image editing utility (Adobe PhotoShop) to separate individual clusters into their own bitmap images and remove any extraneous dark pixels from the background, leaving the clusters situated on a pure white background. This was done by first removing all pixels that fell below a user-defined gray scale threshold and removing remaining material that was not connected to the cluster being analyzed.

These correctly formatted cluster images were analyzed by a program that read each pixel of the image into a two-dimensional array. If the pixel is any color other than white, the program stored it into the array as a "black" pixel contained in the cluster; otherwise, it is considered background, which is white. It is for this reason that all background pixels must be set to pure white before analysis. Once the array was loaded, the program found the center of mass (x_{cm}, y_{cm}) of the cluster by treating all black pixels as equally weighted points on a two-dimensional grid. Once the center of mass was determined, the program calculated

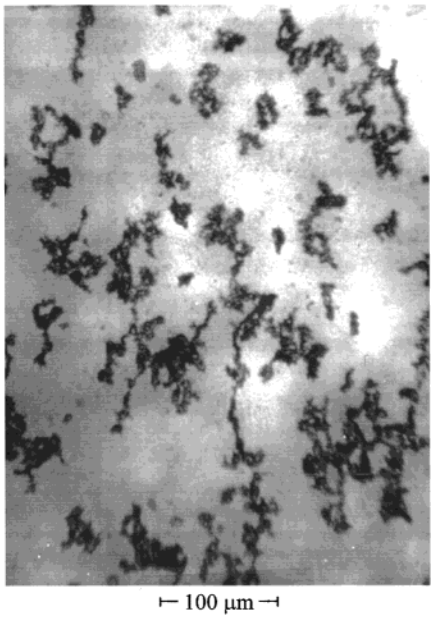

Figure 2. Impaction collected supersoot aggregates from the acetylene air flame 8 cm above the burner orifice.

the radius of gyration of the two-dimension, projected cluster image given by

$$R_g = \Sigma((y - y_{cm})^2 + (x - x_{cm})^2)^{1/2}/N_p \quad (2)$$

where N_p is the total number of black pixels in the cluster image. The program's output was R_g, (x_{cm}, y_{cm}), and N_p.

2.4. Soot Cluster Image Analysis. The fractal dimension of the soot was determined for an ensemble of soot clusters by using the principal relation in eq 1.

A problem relevant to clusters as large as those considered here is that the monomers are too small to be resolved when the whole cluster is viewed. This problem can be overcome, however, by recognizing that the total number of black pixels N_p in the cluster image is proportional to the number of monomers. Thus

$$N_p \sim N \quad (3)$$

This holds as long as the projected image on the two-dimensional plane accurately represents the true three-dimensional aggregate.

For a finite-sized, three-dimensional fractal aggregate, however, it has been found that parts of the cluster can randomly screen other parts during two-dimensional image formation. Thus the projected area, proportional to N_p, does not account for all the material in the cluster. This problem has been well studied by a number of workers to find the useful empirical relation[12,21,22]

$$N \sim N_p^{\alpha} \quad (4)$$

where $\alpha = 1.10 \pm 0.02$ is found empirically for aggregates with $D \sim 1.75$.

Combining eq 1 with either (3) or (4) yields

$$N_p \sim R_g^{D} \quad (5)$$

or

$$N_p \sim R_g^{D/\alpha} \quad (6)$$

(21) Medalia, A. I.; Heckman, F. A. Morphology of aggregates II. Size and shape factors of carbon black aggregates from electron microscopy. *Carbon* **1969**, *7*, 657.

(22) Oh, C.; Sorensen, C. M. The Effect of Monomer Overlap on the Morphology of Fractal Aggregates. *J. Colloid Interface Sci.* **1997**, *193*, 17−25.

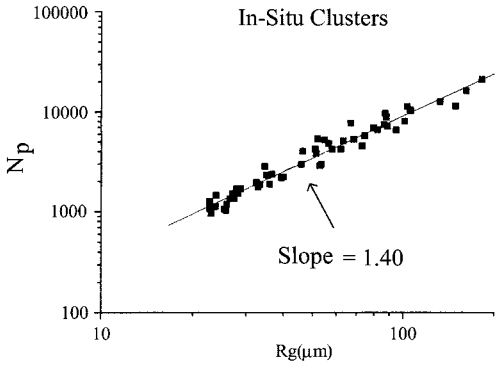

Figure 3. Number of black pixels in an aggregate image versus aggregate projected radius of gyration for in-situ observed soot. The line is a best fit with a slope of 1.40 ± 0.04.

respectively. Equation 5 holds when projection faithfully represents the aggregate, and (6) holds for projection of three-dimensional fractal aggregates with $D \sim 1.75$ onto a two-dimensional image.

This method was tested on artificial, two-dimensional DLCA clusters which can be created by drawing and which have an exact, analytically calculable fractal dimension of $D = 1.440$.[23] Analysis of an ensemble of these artificial clusters with eq 5 yielded $D = 1.44 \pm 0.01$, in exact agreement with the analytical value.

3. Results

3.1. In Situ Aggregates. Figure 3 shows N_p vs R_g data for the soot aggregates photographed in the flame with the telemicroscope, flash lamp arrangement. The data follow a linear relationship on this log−log plot to imply a power law functionality between N_p and R_g. The slope of the plot, hence the power law, is $D = 1.40 \pm 0.04$ found with a linear least-squares fit.

The questions now is whether to correct this value of D for the effects of projection of the aggregate image onto a two-dimensional plane. Visual inspection of the photographs of these in-situ clusters shows the aggregates to be flat; i.e., one of their three dimensions is significantly smaller than the other two. This is apparent in Figure 1, where we see clusters near the center of the photograph face-on and those at the edge of the flame are edge-on and significantly thinner from this perspective. Using the cylindrical coordinates of the flame, we claim the radial dimension of the aggregates is much less than either the azimuthal or axial dimensions. Fractal analysis of the in-situ aggregates was performed only on "face-on" images, i.e., those clusters for which projection onto the image plane occurred along the short, radial direction. Given this, we do not expect any significant intracluster screening and the two-dimensional image to be a faithful representation of the three-dimensional cluster. Thus, the analysis of eq 5 applies, and we conclude the fractal dimension of these flat clusters is $D = 1.40 \pm 0.04$.

It is worthwhile to consider the correction implied by eq 6 applied to these data. Then the fractal dimension would be $D = 1.40\alpha = 1.54$. This, like the value 1.40, is significantly less than $D = 1.75$ expected for three-dimensional DLCA fractal aggregates.

3.2. Impaction-Collected Soot Aggregates. Figure 4 shows N_p vs R_g for the soot aggregates collected via impaction. Again linearity on this log−log plot implies the expected power law functionality; the power law exponent is found to be 1.59 ± 0.05.

(23) Sorensen, C. M.; Oh, C. Divine Proportion Shape Preservation and the Fractal Nature of Cluster-Cluster Aggregates. *Phys. Rev. E* **1998**, *58*, 7545−7548.

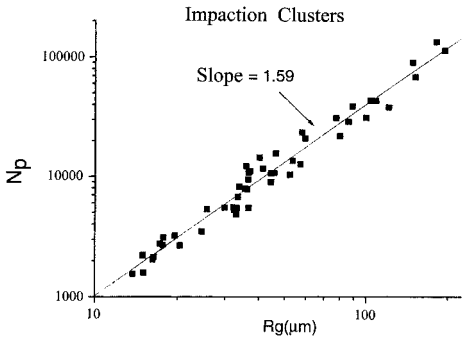

Figure 4. Number of black pixels in an aggregate image versus aggregate projected radius of gyration for impaction-collected soot. The line is a best fit with a slope of 1.59 ± 0.05.

Should the impaction collected clusters be treated as two-dimensional objects unperturbed from their true nature in the flame or does the collection via impaction change their structure? The exponent of the N_p vs R_g power law is 1.59 ± 0.05 significantly different than 1.40 ± 0.04 found in-situ. This implies the structure has changed with collection. It is not unreasonable to propose that if a flat cluster were to impact on the glass slide, it could "crumple", i.e., become bent and hence slightly condensed from the impact. A slightly crushed cluster would have a smaller radius for the same amount of primary particles and would thus have a raised fractal dimension. Furthermore, if the flat cluster were indeed crumbled to a more globular shape, then the analysis of eq 6, which corrects for a three-dimensional object's distortion when projected onto a two-dimension plane, would be appropriate. Then the fractal dimension would be the factor α larger than the measured exponent which yields $D = 1.75 \pm 0.06$. This seems to explain our conclusion in previous work[13] that $D = 1.8$ for these supersoot particles collected via impaction.

It remains to explain the fractal dimension of 1.40 ± 0.04 for the flat, supersoot clusters. The flame photographs, such as Figure 1, show that the supersoot clusters are confined to a cylindrical annulus, thin in the radial direction. "Thin" is a relative term by which we mean relative to the axial and azimuthal dimensions of the cluster. Thus, these cluster can only move in two dimensions. With this, we expect aggregation to proceed in terms of two-dimensional diffusion limited cluster aggregation (DLCA) for which simulations yield an essentially universal value of $D = 1.44 \pm 0.02$.[18,19] This is in excellent agreement with our measured value of D. We remark that before the clusters are large, 100's of micrometers, i.e., when they are submicrometer, the radial dimension is probably not restricted; hence, three-dimensional DLCA occurs and $D = 1.75-1.8$ is expected and, indeed, observed via static light scattering.[20] However, when the size of the soot clusters becomes supermicron, they must find themselves constrained by the thin radial dimension of the flame front causing 2D DLCA to take over. Still remarkable, however, is how fast these supersoot clusters have grown, which, as we have described previously,[20] appears anomalous. Thus a complete understanding of their growth is still lacking. Finally, we think the fact that the fractal dimension of the impaction-collected supersoot falls within the range of that for three-dimensional DLCA clusters is probably entirely coincidental.

4. Conclusion

The in-situ method of observation shows aggregates with a fractal dimension much closer to that associated with two-dimensional DLCA aggregation than that of

three-dimensional DLCA aggregation. Two-dimensional DLCA growth yields a fractal dimension of approximately 1.44 in simulations,[18,19] which is consistent with our measurements which yield a fractal dimension of 1.40 ± 0.04. This result is supported by visual inspection of the clusters, showing them to be held in a thin annulus that restricts the clusters to a quasi-two-dimensional region. In this region, clusters are free to diffuse and aggregate together in only two dimensions, resulting in the growth of two-dimensional DLCA fractal soot clusters.

Acknowledgment. This work was supported by NSF Grant CTS 9709764.

LA0104065